

Rotational spectra of isotopic species of methyl cyanide, CH₃CN, in their $\nu_8 = 1$ excited vibrational states

Holger S. P. Müller¹, Brian J. Drouin², John C. Pearson², Matthias H. Ordu¹, Nadine Wehres¹, and Frank Lewen¹

¹ I. Physikalisches Institut, Universität zu Köln, Zùlpicher Str. 77, 50937 Köln, Germany
e-mail: hspm@ph1.uni-koeln.de

² Jet Propulsion Laboratory, California Institute of Technology, Mail Stop 183-301, 4800 Oak Grove Drive, Pasadena, CA 91011-8099, USA

Received 20 October 2015 / Accepted 27 November 2015

ABSTRACT

Context. Methyl cyanide is an important trace molecule in space, especially in star-forming regions where it is one of the more common molecules used to derive kinetic temperatures.

Aims. We want to obtain accurate spectroscopic parameters of minor isotopologs of methyl cyanide in their lowest excited $\nu_8 = 1$ vibrational states to support astronomical observations, in particular, with interferometers such as ALMA.

Methods. The laboratory rotational spectrum of methyl cyanide in natural isotopic composition has been recorded from the millimeter to the terahertz regions.

Results. Transitions with good signal-to-noise ratios could be identified for the three isotopic species CH₃¹³CN, ¹³CH₃CN, and CH₃C¹⁵N up to about 1.2 THz ($J'' \leq 66$). Accurate spectroscopic parameters were obtained for all three species.

Conclusions. The present data were already instrumental in identifying $\nu_8 = 1$ lines of methyl cyanide with one ¹³C in IRAM 30 m and ALMA data toward Sagittarius B2(N).

Key words. molecular data – methods: laboratory: molecular – techniques: spectroscopic – radio lines: ISM – ISM: molecules – astrochemistry

1. Introduction

The degree of molecular complexity in the interstellar medium (ISM) is particularly large in the warm and dense parts of star-forming regions known as “hot cores” or “hot corinos”. A large number of organic molecules with up to 12 atoms have been detected thus far, for example, in the high-mass star-forming region Sagittarius (Sgr for short) B2(N) (Belloche et al. 2009, 2013, 2014). The Orion KL region is another high-mass star-forming region in which molecular complexity has been studied extensively (e.g., Tercero et al. 2015, and references therein). IRAS 16293-2422 (e.g., Jørgensen et al. 2012; Pineda et al. 2012, and references therein) and NGC 1333-IRAS2A (Maury et al. 2014) are corresponding examples of low-mass star-forming regions. The Molecules in Space webpage¹ of the Cologne Database for Molecular Spectroscopy, CDMS (Müller et al. 2001, 2005) lists molecules detected in various astronomical sources with detailed information in most cases.

Molecular complexity in the ISM is not only manifest in increasingly larger molecules, but also in excited vibrational states or minor isotopologs of abundant smaller molecules. Corresponding laboratory rotational data are not only necessary to be able to avoid confusing such lines with those of larger and rarer molecules, but these data also have certain diagnostic values. Transitions in excited vibrational states may be used to derive a physical model of a particular source, as done, for example, in the case of CRL 618 and vibrationally excited HC₃N isotopologs (Wyrowski et al. 2003). Ratios of isotopic species may

provide clues to the formation of a molecule, such as more in the gas phase or more on grain surfaces, as in the case of dimethyl ether (Koerber et al. 2013), among others.

The ¹²C/¹³C ratio is particularly low in the vicinity of the Galactic center (~20) (Wilson & Rood 1994; Milam et al. 2005; Müller et al. 2008). Thus, it is not surprising that some ¹³C containing saturated organic molecules were detected soon after the main species and mainly toward the Galactic center source Sgr B2. These are H¹³C(O)NH₂ (Lazareff et al. 1978), ¹³CH₃OH (Gottlieb et al. 1979), and CH₃¹³CN (Cummins et al. 1983). Both ¹³C containing CH₃CN isotopomers were detected in a line survey of Orion (Sutton et al. 1985). Detections of molecules containing ¹³C were often hampered by the lack of laboratory data. In recent years, there have been several reports not only on the laboratory spectroscopy of ¹³C containing isotopologs, but also on their detections in space. These include ethyl cyanide (Demyk et al. 2007), vinyl cyanide (Müller et al. 2008), methyl formate (Carvajal et al. 2009), and dimethyl ether (Koerber et al. 2013). The ¹³C containing ethanol isotopomers have also been studied (Bouchez et al. 2012), but only tentatively identified in a line survey of Sgr B2(N) carried out with the IRAM 30 m radio telescope (Belloche et al. 2013). A firm detection has been achieved only very recently (Müller et al. 2016). Further investigations of ¹³C containing organic molecules include acetaldehyde (Margulès et al. 2015), whose detection has not been reported as far as we know, and methanol (Xu et al. 2014).

Methyl cyanide, CH₃CN, also known as acetonitrile or cyanomethane, was among the early molecules to be detected by radio astronomical means. Solomon et al. (1971) detected it

¹ <https://cdms.astro.uni-koeln.de/classic/molecules>

almost 40 years ago toward the massive star-forming regions Sgr A and B close to the Galactic center. The molecule was also detected in its $v_8 = 1$ excited vibrational state ($E_{\text{vib}} = 525$ K and even in $v_8 = 2$ and in $v_4 = 1$ ($E_{\text{vib}} = 1324$ K (Belloche et al. 2013, 2015). Several rarer isotopic species have been detected. They include CH_2DCN in the hot core sources IRC2 in OMC1 and, tentatively, in G34.3 (Gerin et al. 1992) and in Sgr B2(N2) (Belloche et al. 2015). Sgr B2(N2) is to the north of Sgr B2(N1), which is also known as the Large Molecule Heimat (Belloche et al. 2015). Even $^{13}\text{CH}_3^{13}\text{CN}$ was detected in Sgr B2(N), first tentatively (Belloche et al. 2013) and, more recently, with confidence (Belloche et al. 2015). In addition, Belloche et al. (2013, 2015) identified transitions of $\text{CH}_3^{13}\text{CN}$ and $^{13}\text{CH}_3\text{CN}$ in their $v_8 = 1$ excited vibrational states.

Methyl cyanide was also among the first molecules to be studied by microwave spectroscopy (Ring et al. 1947). In their rotational and rovibrational study of $v_8 = 0, 1$, and 2, Müller et al. (2015) revealed and analyzed pronounced interactions between the last two states. In addition, they analyzed an interaction between the first two states. A few years earlier, some of us contributed extensive accounts of the ground vibrational states of several isotopic species of methyl cyanide, including $\text{CH}_3^{13}\text{CN}$, $^{13}\text{CH}_3\text{CN}$, and $\text{CH}_3\text{C}^{15}\text{N}$ (Müller et al. 2009). Bauer & Maes (1969) and Bauer et al. (1975) reported the rotational spectrum of $\text{CH}_3\text{C}^{15}\text{N}$ in its $v_8 = 1$ excited state up to $J = 8 - 7$ below 144 GHz. The only published rotational data of $\text{CH}_3^{13}\text{CN}$ and $^{13}\text{CH}_3\text{CN}$ in their $v_8 = 1$ states were provided by Tam et al. (1988), who measured transitions up to $J = 3 - 2$ below 56 GHz.

We have measured rotational spectra of methyl cyanide in natural isotopic composition both in wide and in more limited frequency windows up to 1.63 THz to provide new or updated catalog entries for various isotopologs of methyl cyanide, as well as for excited vibrational states. In the present article we analyzed these and new spectra to derive spectroscopic parameters of $^{13}\text{CH}_3\text{CN}$, $\text{CH}_3^{13}\text{CN}$, and $\text{CH}_3\text{C}^{15}\text{N}$ in their $v_8 = 1$ excited vibrational states; as usual, unlabeled atoms refer to ^{12}C and ^{14}N . Preliminary results from this study were used to identify lines of the ^{13}C species in 3 mm molecular line surveys of Sgr B2(N) with the IRAM 30 m telescope (Belloche et al. 2013) and with the Atacama Large Millimeter/submillimeter Array (ALMA) (Belloche et al. 2015).

2. Experimental details

All measurements at the Universität zu Köln were recorded at room temperature in static or very slow flow mode, employing a 7 m long double path Pyrex glass cell equipped with Teflon windows and having an inner diameter of 100 mm. The pressure of CH_3CN was in the range of 0.3–0.5 Pa. Source-frequency modulation was used with demodulation at $2f$, causing an isolated line to appear close to a second derivative of a Gaussian.

The $J = 3 - 2$ transitions of $^{13}\text{CH}_3\text{CN}$ and $\text{CH}_3^{13}\text{CN}$ in their $v_8 = 1$ excited vibrational states around 53.8 and 55.3 GHz, respectively, were recorded with an Agilent E8257D microwave synthesizer as source and a Schottky diode detector. In addition, $J = 6 - 5$ transitions of $^{13}\text{CH}_3\text{CN}$ and $\text{CH}_3\text{C}^{15}\text{N}$ around 107.4 GHz and the $J = 5 - 4$ and $6 - 5$ transitions of $\text{CH}_3^{13}\text{CN}$ around 92.2 and 110.6 GHz, respectively, were recorded with essentially the same instrument. Source frequencies were generated using a Virginia Diodes, Inc. (VDI) tripler driven by the synthesizer mentioned above. The measurements were similar to the ones of 1,2-propanediol (Bossa et al. 2014) and mono-deuterated ethanol (Walters et al. 2015) taken at lower frequencies.

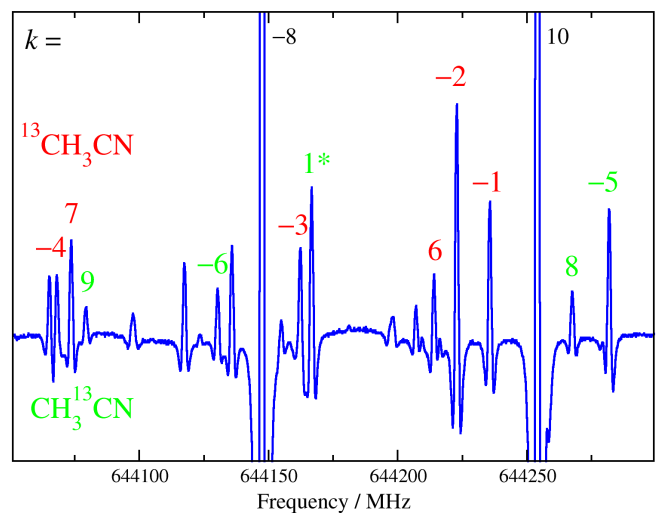


Fig. 1. Section of the submillimeter spectrum of CH_3CN . Transitions of $^{13}\text{CH}_3\text{CN}$ ($J = 36 - 35$) and $\text{CH}_3^{13}\text{CN}$ ($J = 35 - 34$) in their $v_8 = 1$ excited vibrational states were labeled with their k quantum numbers. Spin-statistics cause $k = -2, -5$, and 7 to appear stronger than expected, 1^* indicates the A_2 component of the asymmetry-like split $k = +1$ transition, see section 3 for further details. The clipped lines are the $J = 35 - 34$ $k = -8$ and $k = 10$ transitions of the main isotopolog in $v_8 = 1$. The latter line is overlapping the A_1 component of the $k = +1$ $J = 36 - 35$ line of $\text{CH}_3\text{C}^{15}\text{N}$, $v_8 = 1$. The lines appear similar to second derivatives of a Gaussian line-shape because of the $2f$ -modulation.

We assigned uncertainties from 5 to 20 kHz to these lines because the lines were so narrow at these low frequencies and because of the good signal-to-noise ratios (S/Ns). Hyperfine structure caused by the ^{14}N nucleus was resolved partially for several of these transitions.

The majority of the data were extracted from broad frequency scans taken with the JPL cascaded multiplier spectrometer (Drouin et al. 2005). Generally, a multiplier chain source is passed through a one to two-meter path length flow cell and detected by a silicon bolometer cooled to near 1.7 K. The cell is filled with a steady flow of reagent grade acetonitrile and the pressure and modulation are optimized to enable good S/Ns with narrow lineshapes. With a gas with very strong transitions, such as the $K < 7$ transitions of the main isotopolog of acetonitrile, the S/N was optimized for a higher K transition (e.g., $K = 12$), such that the lower K transitions exhibit saturated line profiles. This procedure enables a better dynamic range for the extraction of line positions for rare isotopologs and highly excited vibrational satellites. The frequency ranges covered most of the 400 to 1200 GHz region. Spectra around 1600 GHz were not considered in the present work because the ground state transitions of the three isotopic species were already too weak to be used in the final fits (Müller et al. 2009). These measurements are similar to recent ones of mono-deuterated ethane (Daly et al. 2015), with one important difference being the very small dipole moment of the ethane isotopolog.

The efficiency of frequency multipliers usually changes strongly with frequency. In addition, recording conditions and sensitivities of detectors can have strong influences on the quality of the spectra. Uncertainties of 50 to 100 kHz were assigned to typical lines. Larger uncertainties of up to 200 kHz were assigned to weaker lines or lines that were not isolated, smaller uncertainties down to 20 kHz for isolated lines with very good S/N and a very symmetric line shape.

3. Results, analyses, and discussion

The basic features of the rovibrational energy level structure of CH₃CN in its three lowest vibrational states ($v_8 \leq 2$) have been given by Müller et al. (2015). The main isotopolog of methyl cyanide and the ones investigated in the present work are prolate symmetric rotors with C_{3v} symmetry. Since the three light H atoms are the only ones not on the symmetry axis, the A rotational parameter is much larger than B , ~ 5.27 cm⁻¹ versus 0.307 cm⁻¹. The rotational energy increases therefore rapidly with K and less so with J . The intensities of transitions involving higher K levels drop quickly in intensity as a consequence. The rotational energies of the highest K levels accessed in the present study correspond to ~ 750 cm⁻¹ or ~ 1080 K. The $\Delta K = 0$ selection rules for rotational transitions cause transitions with the same J to occur in a comparatively narrow frequency range with the spacing increasing quite regularly with K in the ground vibrational state. This is why rotational transitions of CH₃CN are frequently used to infer the temperature in the dense ISM. The spacing between two specific K values also increases with J .

The lowest vibrationally excited state in CH₃CN is the doubly degenerate bending state $v_8 = 1$ with $E_{\text{vib}} = 365$ cm⁻¹ or 525 K for the main isotopic species. Levels having the same K (> 0) repel each other because of the Coriolis interaction, lifting the degeneracy. The K levels in the $l = -1$ stack (i.e., $k = K \times \text{sign}(l) < 0$) are shifted to higher energies, those in the $l = +1$ stack (i.e., $k > 0$) to lower energies. The Coriolis parameter ζ is ~ 0.877 , which is close to the limiting case of $\zeta = 1$, causing levels with $\Delta K = \Delta l = 2$ to be close in energy. The parameter q_{22} causes these levels to repel each other more, because it induces interactions between levels differing in $\Delta K = \Delta l = 2$. The strength of the interaction depends strongly on J , as well as on K . The parameter q_{22} is often abbreviated as q .

These two interactions together lead to a more irregular pattern of the transitions in $v_8 = 1$ with the same J but differing K compared with the quite regular pattern in $v = 0$. Those with $k \leq 0$ occur for lower values of J at decreasing frequencies with fairly regularly increasing spacing. Transitions with $k > 0$ occur less regularly to lower frequencies with $k = +2$ being higher in frequency than $K = 0$. Transitions with $\Delta K = \Delta l = 2$ are often close in frequency at higher K in the absence of additional perturbations. The q_{22} interaction leads to an asymmetry-like A_1/A_2 splitting for the $K = 1, l = +1$ level. The A_1 component is always highest in frequency for each J , whereas the A_2 component occurs near $k = -6$ for lower values of J . Figure 1 shows a part of the rotational spectrum of CH₃CN, in particular with transition of the ¹³C isotopomers in their $v_8 = 1$ excited states.

Spin statistics involving the three equivalent H atoms lead to A and E symmetry levels with *ortho* and *para* spin states, respectively. The K levels with $K - l \equiv 0 \pmod{3}$ have A symmetry with twice the spin weight of the E symmetry K levels with the important exception of $K = 0$ in vibrational (sub-) states with $l \equiv 0 \pmod{3}$, in particular in the ground vibrational state. If the K levels show A_1/A_2 splitting (e.g., $k = +1$ in $v_8 = 1$ of the present CH₃CN isotopologs), each level carries half the spin weight, which means they appear in intensity as if they were E -level transitions.

The large dipole moment of methyl cyanide (3.92197 (13) D, Gadhi et al. 1995) leads to a very strong rotational spectrum, such that CH₂DCN and even ¹³CH₃¹³CN are observable in natural isotopic composition under favorable conditions (Müller et al. 2009). The dipole moment was also determined for CH₃C¹⁵N, yielding an essentially identical value (3.9256 (7) D, Mito et al. 1984a). Dipole moments have also been determined for this iso-

topic species in excited vibrational states (Mito et al. 1984a,b). Excitation to $v_8 = 1$ leads to a value of 3.9073 (13) D.

The terrestrial ¹²C/¹³C and ¹⁴N/¹⁵N ratios are about 90 and 270, respectively (Berglund & Wieser 2011). Transitions in the $v_8 = 1$ excited state are weaker by almost a factor of six than those of the ground vibrational state at room temperature. Thus, CH₃C¹⁵N transitions in $v_8 = 1$ are more than five times stronger than ¹³CH₃¹³CN transitions in $v = 0$. Initially, we searched for transitions of CH₃C¹⁵N because attempts to assign ¹³C isotopomers in their $v_8 = 1$ states in astronomical data (Belloche et al. 2013, 2015) based on the previous laboratory data (Tam et al. 1988) already displayed deviations of up to 2 MHz in the 3 mm wavelength region.

We adjusted the previous $v_8 = 1$ spectroscopic parameters of CH₃C¹⁵N (Bauer & Maes 1969; Bauer et al. 1975) to those used for the main isotopic species (Müller et al. 2015) and estimated higher order parameters for the ¹⁵N species as described below. After fitting the previously reported transition frequencies with their reported uncertainties and creating predictions for higher frequencies, assignments could be made rather easily in the 446–483 GHz region ($J'' = 24 - 26$). Subsequently, we estimated spectroscopic parameters for the CH₃CN isotopomers containing one ¹³C isotope in their $v_8 = 1$ states from their ground-state parameters (Müller et al. 2009), along with the CH₃CN and CH₃C¹⁵N parameters in $v_8 = 0$ and 1. These assignments could be made relatively easily in essentially the same frequency window.

Subsequently, we increased the assignments in several steps to higher J and K values for all three isotopologs. Eventually, the J range covered 24 to 66 (23 to 64 for CH₃¹³CN for which the B value is almost the same as for the main species). Around 20 transition frequencies could be assigned for each k and each of the two ¹³C isotopomers between $k = -6$ and $+10$ with assignments decreasing to higher K because of decreasing intensity. The number of assigned transition frequencies for each k of CH₃C¹⁵N were very similar for the lowest energy k values, but decreased earlier because of the lower abundance of the isotopolog compared to the two with one ¹³C isotope. Assignments reached $k = +13$ and initially $k = -9$ for all three isotopic species. Based on intensities, we expected to be able to assign at least some transitions with $k = -10$ and -11 , but these were not found to be sufficiently close to the predictions. We suspected that these rather weak transitions were perturbed by $K = 10$ and 11 of $v_8 = 2, l = +2$ via a strong $\Delta v_8 = \pm 1, \Delta K = 0, \Delta l = \pm 3$ Fermi resonance with the strongest effects at $K = 14$ for the main isotopic species (Müller et al. 2015). Including estimates of low-order spectroscopic parameters for $v_8 = 2$ and the $v_8 = 1/v_8 = 2$ interaction parameters into the fit, we were able to assign some transitions with $k = -10$ and -11 for all three isotopologs that displayed perturbations of up to 1 MHz and around 2 MHz, respectively. In the late stages of the project, we also made assignments at millimeter wavelengths for the three isotopic species. These covered $J'' = 2, 4$ and 5 transitions for CH₃¹³CN, $J'' = 2$ and 5 for ¹³CH₃CN, and $J'' = 5$ for CH₃C¹⁵N. Hyperfine structure caused by the ¹⁴N nucleus was resolved partially for several of the transitions in the millimeter-wave range.

Prediction and fitting of the rotational spectra were carried out with the Spcat/Spfit program suite (Pickett 1991). In the CH₃C¹⁵N fits, we used the previously recorded laboratory data (Bauer & Maes 1969; Bauer et al. 1975), except for the $J'' = 5$ transition frequencies, which were replaced by our more accurate data. The $v_8 = 1$ and $v_8 = 2^0$ vibrational energies were taken from Duncan et al. (1978) and corrected for the differences with

Table 1. Spectroscopic parameters or differences (Δ) thereof^a of methyl cyanide isotopologs within $v_8 = 1$.

Parameter	CH ₃ CN ^b	CH ₃ ¹³ CN ^c	¹³ CH ₃ CN ^c	CH ₃ C ¹⁵ N ^c
$E(8^1)$	365.024 365 (9)	357.19	364.56	362.41
$\Delta(A - B)$	-115.930 (26)	-115.930	-115.930	-115.930
ΔB	27.530 277 (49)	26.404 860 (112)	26.688 102 (131)	26.865 362 (274)
$\Delta D_K \times 10^3$	-11.46 (48)	-11.46	-11.46	-11.46
$\Delta D_{JK} \times 10^3$	0.987 5 (6)	0.881 1 (24)	0.945 3 (26)	1.008 2 (50)
$\Delta D_J \times 10^6$	95.599 (17)	92.585 (52)	90.693 (41)	90.608 (60)
$\Delta H_K \times 10^6$	14.9 (22)	15.	15.	15.
$\Delta H_{KJ} \times 10^6$	0.034 1 (22)	0.034	0.033	0.033
$\Delta H_{JK} \times 10^9$	2.59 (6)	2.54	2.44	2.43
$\Delta H_J \times 10^{12}$	315.3 (30)	307.3 (74)	278.6 (56)	293.6 (82)
$\Delta L_J \times 10^{15}$	-2.64 (20)	-2.54	-2.35	-2.30
ΔeQq	-0.038 7 (19)	-0.038 7	-0.038 7	n.a.
$eQq\eta$	0.1519 (113)	0.1519	0.1519	n.a.
$A\zeta$	138 656.20 (7)	139 839.99 (39)	138 857.97 (53)	138 554.93 (105)
η_K	10.332 9 (72)	10.420	10.347	10.317
η_J	0.390 469 (7)	0.389 261 (24)	0.371 764 (23)	0.368 215 (34)
$\eta_{KK} \times 10^6$	-834. (41)	-840.	-835.	-833.
$\eta_{JK} \times 10^6$	-34.06 (6)	-32.42 (44)	-32.87 (40)	-32.27 (60)
$\eta_{JJ} \times 10^6$	-2.359 5 (24)	-2.275 0 (52)	-2.147 1 (49)	-2.173 6 (38)
$\eta_{JKK} \times 10^9$	2.59 (17)	2.6	2.5	2.5
$\eta_{JJK} \times 10^9$	0.509 (6)	0.542 (69)	0.425 (70)	0.478
q	17.798 44 (2)	18.212 58 (33)	16.804 42 (35)	16.860 30 (55)
$q_K \times 10^3$	-2.664 5 (111)	-2.726	-2.516	-2.524
$q_J \times 10^6$	-63.842 (14)	-64.581 (175)	-58.745 (164)	-58.664 (248)
$q_{JK} \times 10^9$	93.19 (53)	95.2	85.4	85.6
$q_{JJ} \times 10^{12}$	311.5 (15)	304.8 (252)	301.0 (218)	257.3 (327)
rms error	0.802	0.808	0.766	0.826

Notes. ^a All parameters in MHz units except $E(8^1)$ in cm^{-1} ; the rms errors of the fits are unitless. Numbers in parentheses are one standard deviation in units of the least significant figures. Parameters without quoted uncertainties were estimated and kept fixed in the analyses; see also section 3. ^b From Müller et al. (2015). ^c This work. Ground state parameters for corresponding isotopolog kept fixed to values in Table 2. Parameters in Table 3 were also used in the analyses.

respect to values determined for the main species by Müller et al. (2015). The correction was only 0.02 cm^{-1} in the latter case because the sharp Q branch of the parallel $2v_8^0$ band permit accurate determinations of the vibrational energies. The absence of a single sharp Q branch in the perpendicular v_8 band led to a larger correction of 0.31 cm^{-1} . Scaling of the vibrational energies of $v_8 = 2^0$ with the ratio $E(v_8 = 2^2)/E(v_8 = 2^0)$ of the main isotopolog was used to estimate $E(v_8 = 2^2)$ values for the three minor isotopic species.

The purely axial parameters A (or $A - B$), D_K , H_K , etc., of a symmetric top molecule cannot be determined by rotational spectroscopy in the absence of perturbations. Moreover, rovibrational spectroscopy is only able to determinethe differences with respect to the ground vibrational state unless ground-state $\Delta K = 3$ loops are formed from rovibrational spectra involving two degenerate states, as was done initially for CH₃CN (Anttila et al. 1993), or through perturbations, or through a combination of both, which we used in our study on $v_8 \leq 2$ states of the main isotopolog (Müller et al. 2015).

The ground-state spectroscopic parameters of the minor isotopic species were initially taken from Müller et al. (2009). Because of slight changes in the ground-state parameters of CH₃CN in our recent study (Müller et al. 2015), we adjusted the purely axial parameters, as well as the estimates of some higher order parameters, and redetermined the remaining ground-state spec-

troscopic parameters from the data in Müller et al. (2009). Initial $v_8 = 1$ spectroscopic parameters of CH₃¹³CN and ¹³CH₃CN or changes thereof, as well as higher order values of CH₃C¹⁵N, were derived from corresponding values of CH₃CN by scaling them with appropriate powers of the ratio of the B rotational constants, as was done earlier for the ground vibrational data (Müller et al. 2009). Later, the distortion corrections η to $A\zeta$ were also scaled with the $A\zeta$ ratio, and the distortion corrections to q were scaled equivalently. Later, lower order spectroscopic parameters of $v_8 = 2$ were estimated in a similar way. The Fermi parameter F , which described the $\Delta v_8 = \pm 1$, $\Delta K = 0$, $\Delta l = \pm 3$ interaction between $v_8 = 1$ and 2, was assumed to be identical for all isotopologs. The hyperfine structure was reproduced well by the ground-state parameters of the respective isotopologs combined with the changes from the ground to the $v_8 = 1$ state of the main isotopic species.

Throughout, we tried to fit the rotational spectra of the three methyl cyanide isotopologs with as few spectroscopic parameters being floated as possible. Starting from the lowest order parameters, we searched at each intermediate fit for the parameter that reduced the rms error (also known as the reduced or weighted χ squared) of the fit most. The rms error of the fit is a measure of the quality of the fit, and it should be close to 1.0 ideally, preferably slightly smaller. We tried to avoid floating parameters that changed from the initial value by too much.

Table 2. Ground-state spectroscopic parameters^a (MHz) of methyl cyanide isotopologs.

Parameter	CH ₃ CN ^b	CH ₃ ¹³ CN ^c	¹³ CH ₃ CN ^c	CH ₃ C ¹⁵ N ^c
(A – B)	148 900.103 (66)	148 904.65	149 165.69	149 176.96
B	9 198.899 167 (11)	9 194.349 998 (27)	8 933.309 429 (28)	8 922.038 646 (72)
D _K × 10 ³	2 830.6 (18)	2 831.	2 831.	2 831.
D _{JK} × 10 ³	177.407 87 (25)	176.673 95 (132)	168.239 71 (130)	168.938 71 (336)
D _J × 10 ⁶	3 807.576 (8)	3 809.737 (37)	3 624.947 (32)	3 555.251 (45)
H _K × 10 ⁶	164.6 (66)	165.	165.	165.
H _{KJ} × 10 ⁶	6.062 0 (14)	6.004 5 (131)	5.803 0 (141)	5.647 6 (181)
H _{JK} × 10 ⁹	1 025.69 (15)	1 017.45 (86)	927.19 (86)	951.05 (131)
H _J × 10 ¹²	–237.4 (21)	–258.4 (61)	–273.3 (49)	–183.1 (67)
L _{KKJ} × 10 ¹²	–444.3 (25)	–444.	–431.	–444.
L _{JK} × 10 ¹²	–52.75 (51)	–49.75 (236)	–49.66 (266)	–49.6
L _{JJK} × 10 ¹²	–7.901 (32)	–7.214 (141)	–6.887 (128)	–7.057 (182)
L _J × 10 ¹⁵	–3.10 (17)	–3.10	–2.76	–2.74
P _{JK} × 10 ¹⁵	0.552 (68)	0.55	0.51	0.50
P _{JJK} × 10 ¹⁸	55.3 (22)	55.	49.	49.
eQq	–4.223 08 (107)	–4.218 28 (176)	–4.218 30 (197)	n.a.
C _{bb} × 10 ³	1.845 (90)	1.844	1.792	
(C _{aa} – C _{bb}) × 10 ³	–1.15 (31)	–1.15	–1.10	

Notes. ^a Numbers in parentheses are one standard deviation in units of the least significant figures. Parameters without quoted uncertainties have been estimated from the main isotopic species and were kept fixed in the fits; see section 3. ^b From Müller et al. (2015). ^c From Müller et al. (2009); adjusted in this work to account for slight changes in the parameters of the main isotopolog from that work compared to those in Müller et al. (2015).

Table 3. Low-order spectroscopic parameters or differences (Δ) thereof^a of methyl cyanide describing the Fermi interaction between $\nu_8 = 1$ and $\nu_8 = 2$.

Parameter	CH ₃ CN ^b	CH ₃ ¹³ CN ^c	¹³ CH ₃ CN ^c	CH ₃ C ¹⁵ N ^c
E(8 ²⁰)	716.750 42 (13)	701.10	715.82	711.53
Δ(A – B)	–187.404 (18)	–187.4	–187.4	–187.4
ΔB	54.057 316 (111)	51.856	52.411 5	52.759 1
E(8 ²²)	739.148 225 (56)	723.01	738.19	733.76
Δ(A – B)	–259.956 (122)	–260.0	–260.0	–260.0
ΔB	54.502 729 (70)	52.283 3	52.843 35	53.193 85
Aζ	138 656.042 (102)	139 829.5	138 858.	138 555.
q	17.729 857 (138)	18.141 2	16.738 2	16.794 9
F(8 ^{±1} , 8 ^{2,±2})	53 157.7 (33)	54 567. (744)	51 647. (1303)	51 298. (2967)
F _K (8 ^{±1} , 8 ^{2,±2})	–6.	–6.	–6.	–6.
F _J (8 ^{±1} , 8 ^{2,±2})	–0.369 89 (44)	–0.370	–0.359	–0.359
F _{JJ} (8 ^{±1} , 8 ^{2,±2}) × 10 ⁶	1.681 (87)	1.70	1.58	1.58

Notes. ^a All parameters in MHz units except E(8²⁰) and E(8²²) in cm^{–1}. Numbers in parentheses are one standard deviation in units of the least significant figures. Parameters without quoted uncertainties were estimated and kept fixed in the analyses; see also section 3. ^b From Müller et al. (2015). ^c This work. Ground state parameters for corresponding isotopolog kept fixed to values in Table 2.

Initially, our fits did not include any distortion corrections to F . However, we were unable to reproduce transitions with $k = -10$ and -11 satisfactorily. Floating F yielded relatively small changes from the initial values compared to floating other parameters, but the values were increased by about 15 % to 20 %. Trial fits, with fixed F_J values scaled with the ratio of the B rotational constants included, reduced the values of F to around that of the main isotopic species. Even though including F_K and F_{JJ} had effects within the uncertainties of F , they were retained in the fits. The final set of $\nu_8 = 1$ spectroscopic parameters of the

three methyl cyanide isotopic species is given in Table 1, along with values for the main species from Müller et al. (2015). The adjusted ground-state parameters are provided in Table 2. These parameters were kept fixed in all $\nu_8 = 1$ fits. Finally, the low-order $\nu_8 = 2$ parameters are summarized in Table 3, along with those describing the Fermi interaction between $\nu_8 = 1$ and 2.

The rms errors of all fits are around 0.8, so the experimental transition frequencies have been reproduced within uncertainties on average, and the uncertainties even appear to be slightly conservative. The $\nu_8 = 1$ parameters in Table 1 are quite similar

among the isotopic species, in particular those of $^{13}\text{CH}_3\text{CN}$ and $\text{CH}_3\text{C}^{15}\text{N}$, which have rather similar vibrational energies and values of ΔB , $A\zeta$, and q . The ground-state parameters of three minor isotopic species change only slightly with respect to our previous values because of relatively modest changes in the estimates of P_{JK} and somewhat larger changes in L_J . The change in H_K has no effect on the not purely axial parameters. The only floated parameter in Table 3 is the main Fermi term F . The values of the minor isotopic species differ slightly from those of the main species. Assumptions on the purely axial parameters, as well as the truncation of the $v_8 = 2$ parameters, may have non-negligible effects on its values. On the other hand, Müller et al. (2015) pointed out that F appeared to scale roughly with q for the isoelectronic molecules CH_3CN , CH_3CCH (Pracna et al. 2004) and CN_3NC (Pracna et al. 2011). Interestingly, q and F of $\text{CH}_3^{13}\text{CN}$ are both slightly greater than the values of the main species, whereas both are less by very similar amounts for $^{13}\text{CH}_3\text{CN}$ and $\text{CH}_3\text{C}^{15}\text{N}$, and, remarkably, basically identical with $q = 16.78926$ (19) MHz and $F = 51745$ (3) MHz of CH_3CCH (Pracna et al. 2004). However, the agreement with the CH_3CCH values may be coincidental.

4. Conclusion

We have analyzed rotational transitions for three minor isotopologs of methyl cyanide in their $v_8 = 1$ excited vibrational states up to 1.2 THz and combined these data with existing ones in the case of $\text{CH}_3\text{C}^{15}\text{N}$. While the prospects of detecting such lines for this isotopic species are uncertain at present, transitions pertaining to $^{13}\text{CH}_3\text{CN}$ and $\text{CH}_3^{13}\text{CN}$ have already been identified in astronomical spectra with the help of preliminary results from this study (Belloche et al. 2013, 2015).

Predictions generated from the present data should be sufficient for observations with ALMA, and even more so with other arrays or single-dish radio telescopes. These predictions will be available in the catalog section² of the Cologne Database for Molecular Spectroscopy³ (Müller et al. 2001, 2005). The complete line, parameter, and fit files will be deposited in the Spectroscopy Data section of the CDMS. Updated or new JPL catalog (Pickett et al. 1998) entries⁴ will also be available.

The very good S/N of our spectra should permit analyses of rotational transitions of $^{13}\text{CH}_3\text{CN}$ and $\text{CH}_3^{13}\text{CN}$, possibly even of $\text{CH}_3\text{C}^{15}\text{N}$ in their $v_8 = 2$ and $v_4 = 1$ excited vibrational states. Such transitions may well be detectable in astronomical spectra in case of the ^{13}C containing isotopomers.

The use of enriched samples will permit accessing energy levels having even higher J and K quantum numbers, which will yield an improved description of the $v_8 = 1$ and 2 interactions. However, such a study will also require recording and analyses of v_8 and $2v_8$ infrared spectra.

Acknowledgements. The measurements in Köln were supported by the Deutsche Forschungsgemeinschaft (DFG) through the collaborative research grant SFB 956, project area B3. We would like to thank Dr. Bernd Vowinkel for making Schottky detectors available for our measurements. The portion of this work, which was carried out at the Jet Propulsion Laboratory, California Institute of Technology, was performed under contract with the National Aeronautics and Space Administration (NASA).

References

- Anttila, R., Horneman, V.-M., Koivusaari, M. & Paso, R. 1993, *J. Mol. Spectrosc.*, 157, 198
- Bauer, A., & Maes, S. 1969, *J. Phys. (Paris)*, 30, 169
- Bauer, A., Tarrago, G., & Remy, A. 1975, *J. Mol. Spectrosc.*, 58, 111
- Belloche, A., Garrod, R. T., Müller, H. S. P., et al. 2009, *A&A*, 499, 215
- Belloche, A., Müller, H. S. P., Menten, K. M., Schilke, P., & Comito, C. 2013, *A&A*, 559, A47
- Belloche, A., Garrod, R. T., Müller, H. S. P., & Menten, K. M. 2014, *Science*, 345, 1584
- Belloche, A., Müller, H. S. P., Garrod, R. T., & Menten, K. M. 2016, *A&A*, 587, A91
- Berglund, M.; & Wieser, M. E. 2011, *Pure Appl. Chem.*, 83, 397
- Bossa, J.-B., Ordu, M. H., Müller, H. S. P., Lewen, F., & Schlemmer, S. 2014, *A&A*, 570, A12
- Bouchez, A., Walters, A., Müller, H. S. P., et al. 2012, *J. Quant. Spectrosc. Radiat. Transfer*, 113, 1148
- Carvajal, M., Margulès, L., Tercero, B., et al. 2009, *A&A*, 500, 1109
- Cummins, S. E., Green, S., Thaddeus, P., & Linke, R. A. 1983, *ApJ*, 266, 331
- Daly, A. M., Drouin, B. J., Groner, P., Yu, S., & Pearson, J. C. 2015, *J. Mol. Spectrosc.*, 307, 27
- Demyk, K., Mäder, H., Tercero, B., et al. 2007, *A&A*, 466, 255
- Drouin, B. J., Maiwald, F. W., & Pearson, J. C. 2005, *Rev. Sci. Instr.*, 76, 093113
- Duncan, J. L., McKean, D. C., Tullini, F., Nivellini, G. D., & Perez Peña, J. 1978, *J. Mol. Spectrosc.*, 69, 123
- Gadhi, J., Lahrouni, A., Legrand, J., & Demaison, J. 1995, *J. Chim. Phys. Phys.-Chim. Biol.*, 92, 1984
- Gerin, M., Combes, F., Wlodarczak, et al. 1992, *A&A*, 259, L35
- Gottlieb, C. A., Ball, J. A., Gottlieb, E. W., & Dickinson, D. F. 1979, *ApJ*, 227, 422
- Koerber, M., Bisschop, S. E., Endres, C. P., et al. 2013, *A&A*, 558, A112
- Jørgensen, J. K., Favre, C., Bisschop, S. E., et al. 2012, *ApJ*, 757, L4
- Lazareff, B., Lucas, R., & Encrenaz, P. 1978, *A&A*, 70, L77
- Margulès, L., Motiyenko, R. A., Ilyushin, V. V., & Guillemin, J. C. 2015, *A&A*, 579, A46
- Maurly, A. J., Belloche, A., André, P., et al. 2014, *A&A*, 563, L2
- Milam, S. N., Savage, C., Brewster, M. A., Ziurys, L. M., & Wyckoff, S. 2005, *ApJ*, 634, 1126
- Mito, A., Sakai, J., & Katayama, M. 1984a, *J. Mol. Spectrosc.*, 103, 26
- Mito, A., Sakai, J., & Katayama, M. 1984b, *J. Mol. Spectrosc.*, 105, 410
- Müller, H. S. P., Thorwirth, S., Roth, D. A., & Winnewisser, G. 2001, *A&A*, 370, L49
- Müller, H. S. P., Schlöder, F., Stutzki, J., & Winnewisser, G. 2005, *J. Mol. Struct.*, 742, 215
- Müller, H. S. P., Belloche, A., Menten, K. M., et al. 2008, *J. Mol. Spectrosc.*, 251, 319
- Müller, H. S. P., Drouin, B. J., & Pearson, J. C. 2009, *A&A*, 506, 1487
- Müller, H. S. P., Brown, L. R., Drouin, B. J., et al. 2015a, *J. Mol. Spectrosc.*, 312, 22
- Müller, H. S. P., Belloche, A., Xu, L.-H., et al. 2016, *A&A*, 587, A92
- Pickett, H. M. 1991, *J. Mol. Spectrosc.*, 148, 371
- Pickett, H. M., Poynter, R. L., Cohen, E. A., et al. 1998, *J. Quant. Spectrosc. Radiat. Transfer*, 60, 883
- Pineda, J. E., Maurly, A. J., Fuller, G. A., et al. 2012, *A&A*, 544, L7
- Pracna, P., Müller, H. S. P., Klee, S., & Horneman, V.-M. 2004, *Mol. Phys.*, 102, 1555
- Pracna, P., Urban, J., Votava, O., et al. 2011, *Mol. Phys.*, 109, 2237
- Ring, H., Edwards, H., Kessler, M., & Gordy, W. 1947, *Phys. Rev.*, 72, 1262
- Solomon, P. M., Jefferts, K. B., Penzias, A. A., & Wilson, R. W. 1971, *ApJ*, 168, L107
- Sutton, E. C., Blake, G. A., Masson, C. R., & Phillips, T. G. 1985, *ApJS*, 58, 341
- Tam, H., An, I., & Roberts, J. A. 1988, *J. Mol. Spectrosc.*, 129, 202
- Tercero, B., Cernicharo, J., López, A., et al. 2015, *A&A*, 582, L1
- Walters, A., Schäfer, M., Ordu, M. H., et al. 2015, *J. Mol. Spectrosc.*, 314, 6
- Wilson, T. L., & Rood, R. 1994, *ARA&A*, 32, 191
- Wyrowski, F., Schilke, P., Thorwirth, S., Menten, K. M., & Winnewisser, G. 2003, *ApJ*, 586, 344
- Xu, L.-H., Lees, R. M., Hao, Y., et al. 2014, *J. Mol. Spectrosc.*, 303, 1

² website: <https://cdms.astro.uni-koeln.de/classic/entries/>, see also <https://cdms.astro.uni-koeln.de/classic/>

³ website: <https://cdms.astro.uni-koeln.de/>

⁴ website: <http://spec.jpl.nasa.gov/ftp/pub/catalog/catdir.html>, see also <http://spec.jpl.nasa.gov/>